Supporting Information for

Covalent Organic Framework-Regulated Ionic Transportation for High-Performance Lithium-Ion Batteries

Yucheng Wen,[a§] Xianshu Wang,[a§] Yan Yang,[a§] Mingzhu Liu,[a] Wenqiang Tu,[a] Mengqing Xu,[ab] Gengzhi Sun,[ab] Seigou Kawaguchi,[c] Guozhong Cao,*[d] and Weishan Li,*[ab]

[a.]School of Chemistry and Environment, South China Normal University, Guangzhou 510006, China.

[b.]National and Local Joint Engineering Research Center of MPTES in High Energy and Safety LIBs, Engineering Research Center of MTEES (Ministry of Education), and Key Lab. of ETESPG (GHEI), South China Normal University, Guangzhou 510006, China.

[c.]Department of Organic Materials Science, Yamagata University, Yonezawa 992-8510, Japan.

[d.]Department of Materials Science and Engineering, University of Washington, Seattle, Washington 98195, United States.

*Corresponding authors, email: gzcao@u.washington.edu; liwsh@scnu.edu.cn

§ These authors equally contributes to this work.

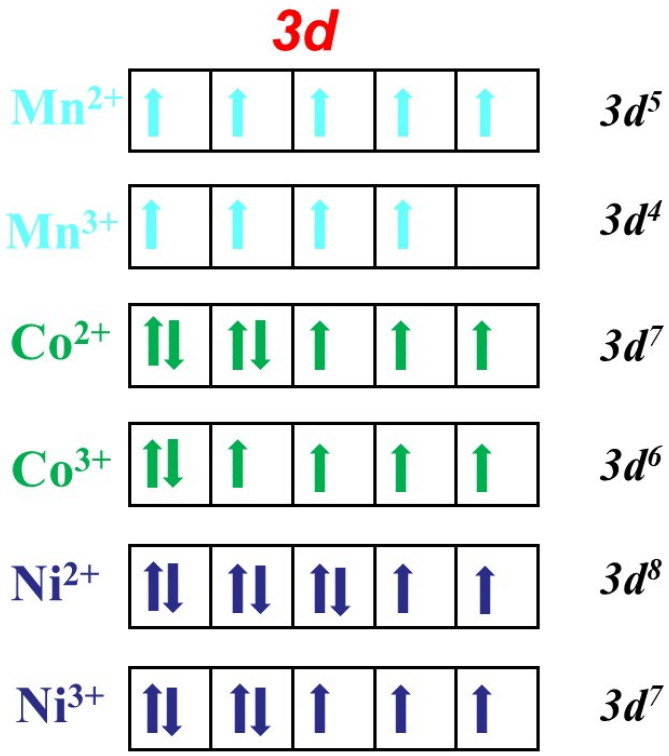

Figure S1. Electronic arrangement of transition metal ions on 3d orbit.

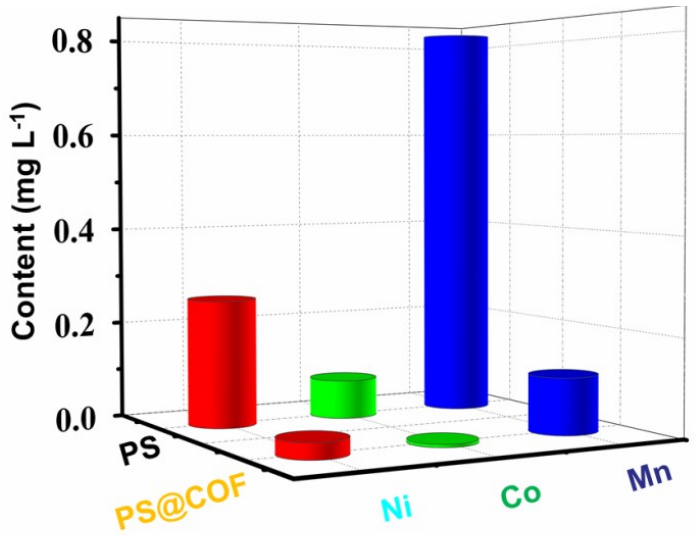

Figure S2. TMI contents detected on on lithium anode of $Li[Li_{0.2}Mn_{0.55}Ni_{0.15}Co_{0.1}]O_2$/Li coin cells after 1000 cycles. The cells were charged and discharged between 4.8 and 2 V (vs. Li/Li^+) at 0.1 C (1 C= 200 mA h g^{-1}) for the first three cycles and at 0.5 C for the remaining cycles.

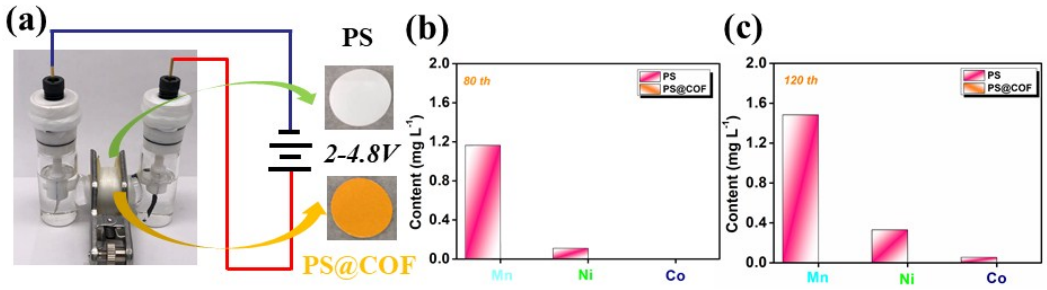

Figure S3. TMI contents detected on Li anode after cycling (a) H-type $Li[Li_{0.2}Mn_{0.55}Ni_{0.15}Co_{0.1}]O_2$/Li cell voltammetrically between 2 and 4.8 V (vs. Li/Li^+) under 0.1 mV s^{-1} for (b) 80 and (c) 120 times

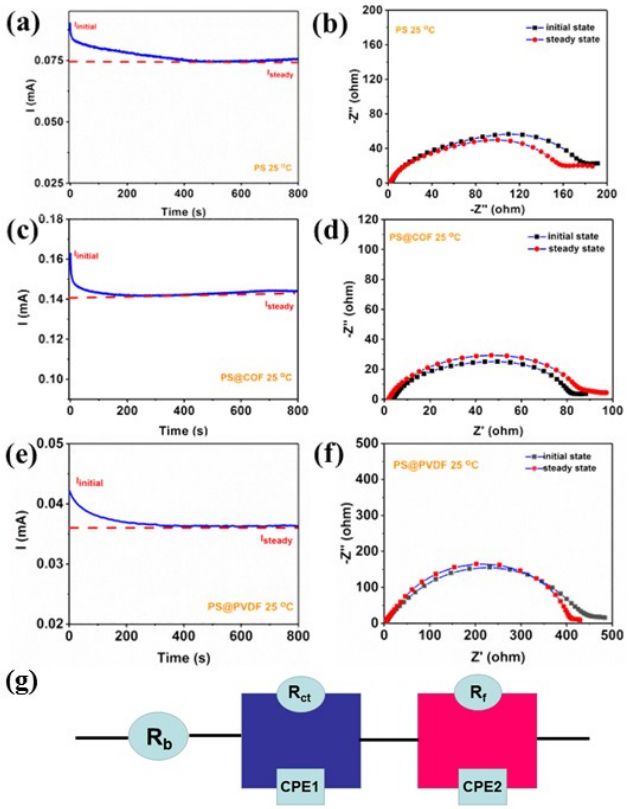

Figure S4. Chronoamperometric responses under a polarization of 20 mV and electrochemical impedance spectra before and after polarization for the Li/Li cells using (a,b) PS, (c,d) PS@COF and (e,f) PS@PVDF. (g) Equivalent circuit for fitting the electrochemical impedance spectra.

T= 25°C

	$I_{initial}$ (mA)	I_{steady} (mA)	$R_{int}^{initial}$ (Ω)	R_{int}^{steady} (Ω)	t_{Li^+}	$t_{PF_6^-}$
PS	0.09015	0.07519	185.03	168.63	0.38	0.62
PS@COF	0.16279	0.14399	81.54	84.76	0.76	0.24
PS@PVDF	0.04229	0.03627	445.36	413.9	0.20	0.80

Table S1. Li^+ transference numbers in different separators, determined from Vincent-Bruce Equation

The determination of Li^+ transference number is based on Vincent-Bruce Equation:[1, 2]

$$t_{Li^+} = \frac{I_{steady} \times (V - I_{initial} \times R_{int}^{initial})}{I_{initial} \times (V - I_{steady} \times R_{int}^{steady})}$$

where $I_{initial}$ and I_{steady} represent initial current and steady-state current recorded during potentiostatic polarization (Fig.S4a,c,e), $R_{int}^{initial}$ and R_{int}^{steady} represent the interfacial resistances before and after polarization, obtained from fitting the electrochemical

impedance spectra (Fig. S4b,d,f) with the equivalent circuit (Fig. S4g). In Fig. S4g, R_b represents solution bulk resistance, while R_{ct} and R_f are the resistances of charge transfer and the film on electrode, respectively. Therefore, the interfacial resistance is the sum of R_{ct} and R_f. The obtained Li^+ transference numbers are presented in Table S1.

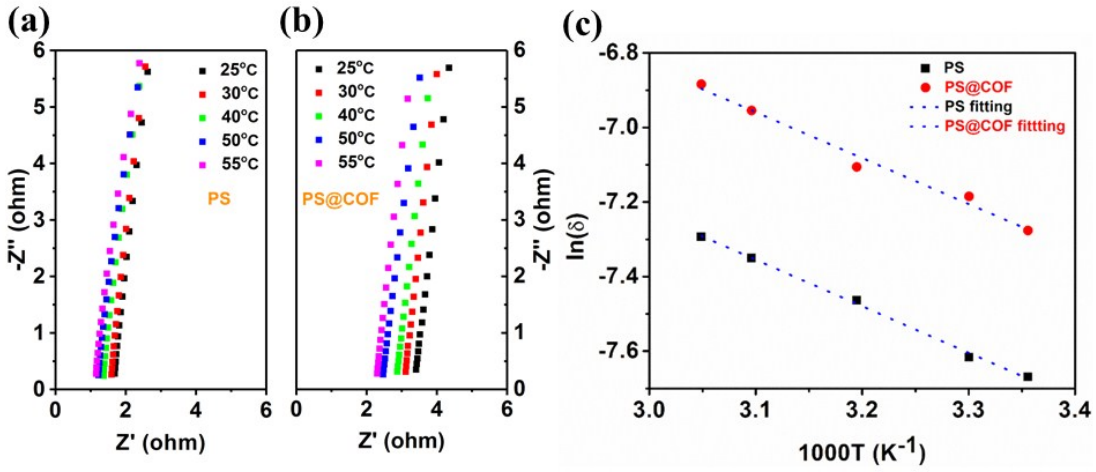

Figure S5. Electrochemical impedance spectra of SS/SS cells with (a) PS and (b) PS@COF. (c) Ionic conductivity at various temperatures and linear fitting with the Arrhenius equation.

	PS (d=20 μm)		PS@COF (d=60 μm)	
Temperature (°C)	R_b (Ω)	δ (mS cm^{-1})	R_b (Ω)	δ (mS cm^{-1})
25	1.68273	0.46707	3.40888	0.69168
30	1.59606	0.49243	3.11099	0.75791
45	1.37016	0.57362	2.87549	0.81998
50	1.22402	0.64211	2.47129	0.95410
55	1.15583	0.67999	2.30181	1.02435

Table S2. Ionic conductivity based on electrochemical impedance spectroscopy.

Symmetrical stainless steel cell, SS/PS/SS and SS/PS@COF/SS, were assembled to measure the ionic conductivity (δ) of the separators based on electrochemical impedance spectroscopy:

$$\delta = \frac{d}{R_b S}$$

where R_b is the bulk resistance, the the value at the intersect of spectra (Fig. S5a,b) with X-axis at high frequency, d and S are the thickness and area of the separator, respectively. The obtained results are presented in Table S2. Apparently, the ionic conductivity of the PS can be highly

improved by coating COF. At ambient temperature (25°C), PS@COF exhibits an ionic conductivity of 0.692 mS cm^{-1} compared to the 0.467 mS cm^{-1} of PS. The relationship of ionic conductivity with temperature follows Arrhenius equation (Fig. S5c).

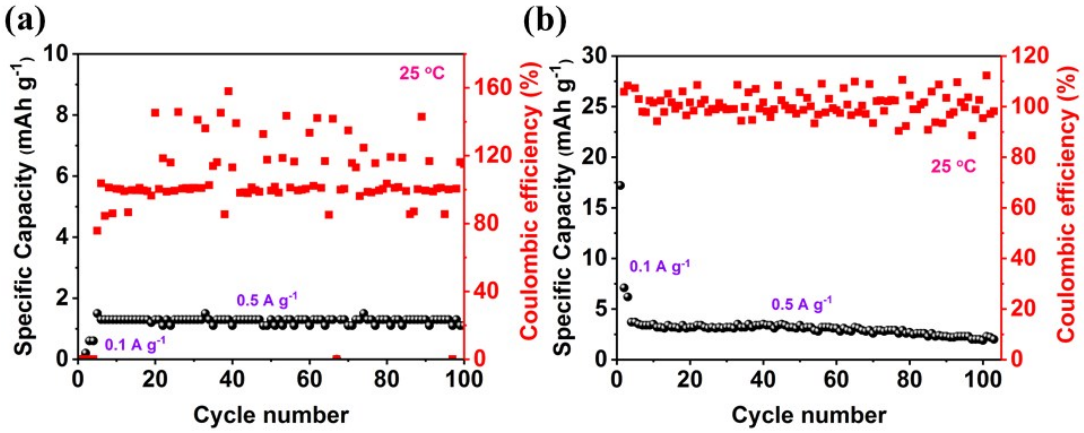

Figure S6. Charge/discharge performances of COF as (a) cathode and (b) anode in COF/Li cells.

COF electrodes were prepared and COF/Li cells were setup to test the charge/discharge performance of COF as anode and cathode in LIBs, using Cu and Al foils as current collectors, respectively. The cells were charged/discharged at 0.1 A g^{-1} COF for initial three cycles and at 0.5 A g^{-1} for the subsequent cycles, between 0 and 3 V for anode and between 2 and 4.8 V for cathode. The obtained results are presented in Fig. S6, which shows that COF electrode exhibits low specific capacity as either anode or cathode. These low capacities originated from the conductive carbon in the electrode, suggesting that COF does not exhibit lithium storage property and is electrochemically stable between 0 and 4.8 V.

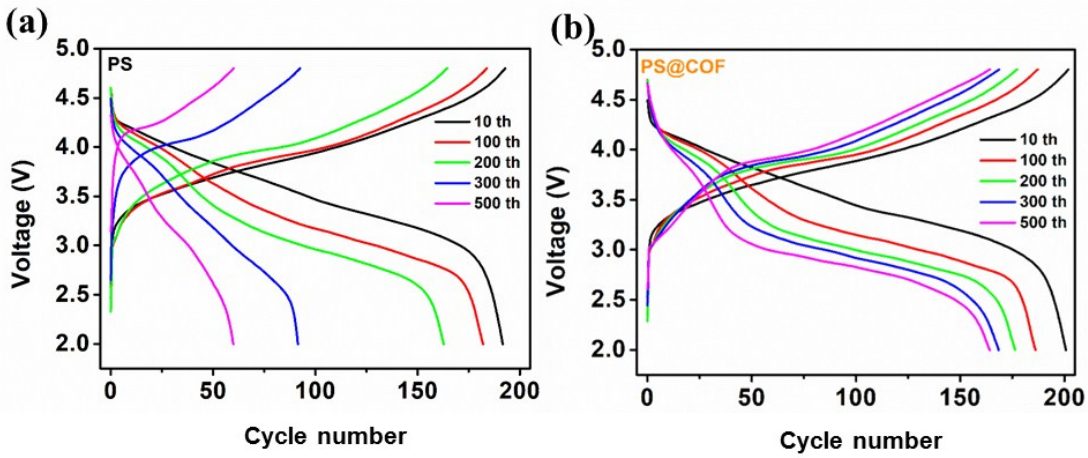

Figure S7. Selected discharge profiles of $Li[Li_{0.2}Mn_{0.55}Ni_{0.15}Co_{0.1}]O_2$/Li cells with (a) PS and (b) PS@COF at 0.5 C.

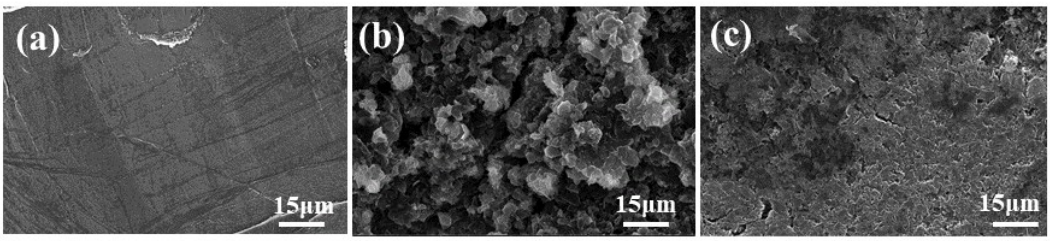

Figure S8. SEM images of fresh Li electrode (a) and the cycled Li electrodes in $Li[Li_{0.2}Mn_{0.55}Ni_{0.15}Co_{0.1}]O_2$/Li cells with (b) PS and (c) PS@COF after 500 cycles

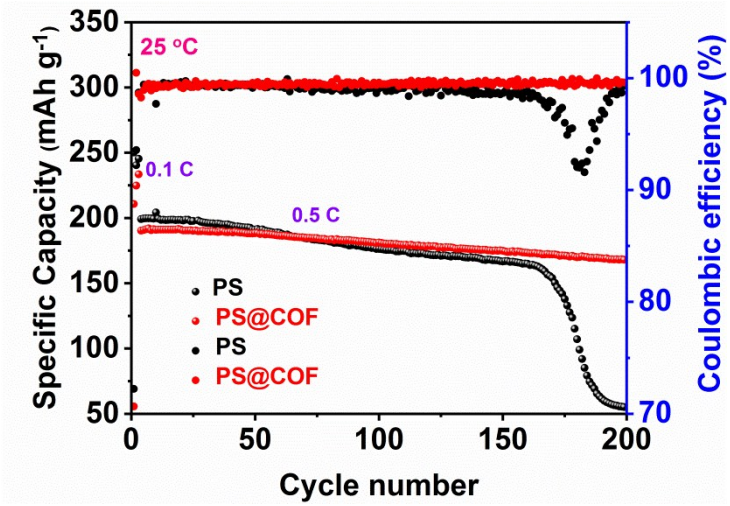

Figure S9. Cycling performance of $Li[Li_{0.2}Mn_{0.55}Ni_{0.15}Co_{0.1}]O_2$/Li cells using PS and PS@COF with 5 μL electrolyte at 0.5 C.

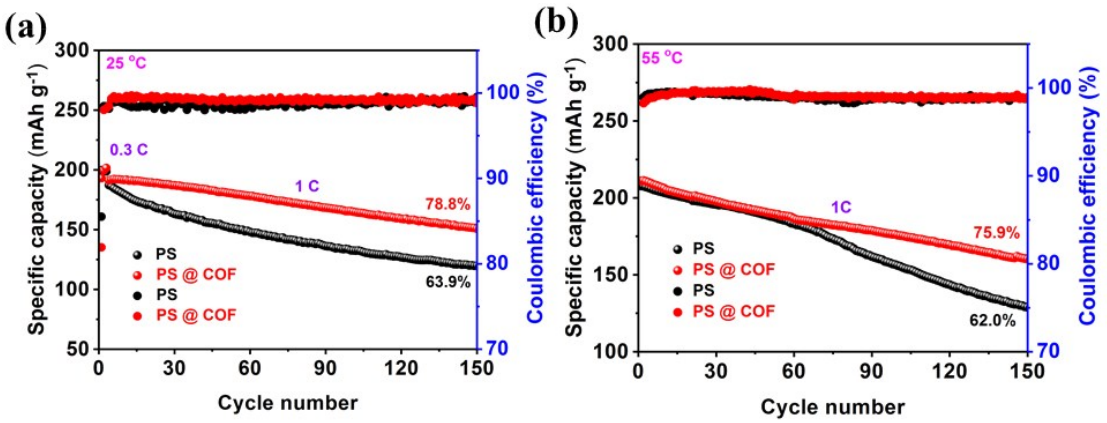

Figure S10. Cyclic performance of NCM811/Li cells with PS and PS@COF at (a) 25°C and (b) 55°C.

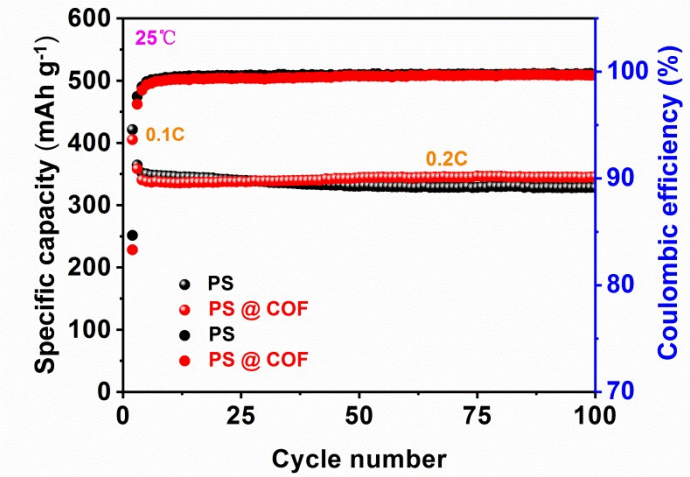

Figure S11. Cycling performance of graphite/Li cells with PS and PS@COF.

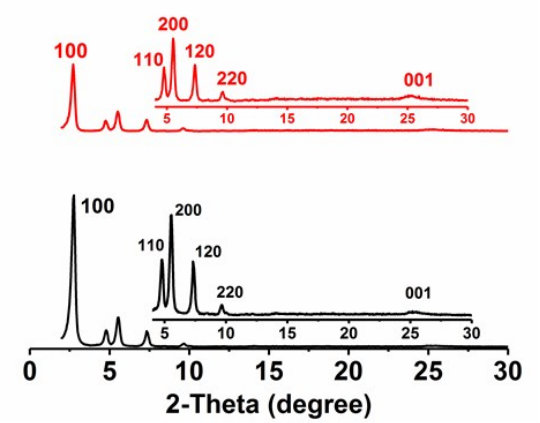

Figure S12. XRD patterns of COF before (black) and after (red) cycling.

TPB-DMTP-COF exhibits the peaks at 2.76°, 4.76°, 5.58°, 7.40°, 9.68°, and 25.2°, corresponding to the (100), (110), (200), (210), (220), and (001) facets.

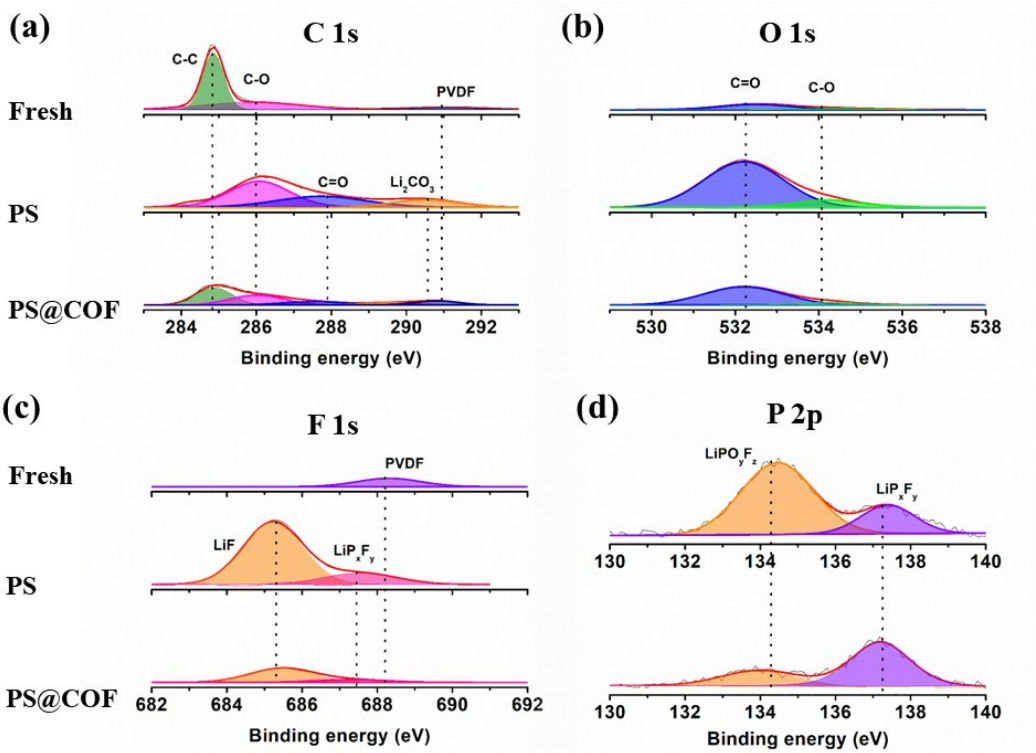

Figure S13. XPS profiles of (a) C 1s, (b) O 1s, (c) P 2p and (d) F 1s on graphite anode from $Li[Li_{0.2}Mn_{0.55}Ni_{0.15}Co_{0.1}]O_2$/graphite full cell before cycling (top) and after cycling with PS (middle) and PS@COF (down) for 500 times.

The C 1s spectra of the fresh graphite electrode contain three main peaks, corresponding to C-C (284.7 eV), and C-F (290.9 eV) in PVDF binder, and the peak of C-O at 286.0 eV.[3] The peak of Li_2CO_3 at 290.4 eV can be observed on graphite with PS, while it almost vanishes for graphite with PS@COF, revealing that the decomposition of the electrolyte is suppressed by COF. C=O (532.3 eV) and C-O (534.1 eV)[4] are detected on the fresh graphite electrode in O 1s spectra. These peaks are more obvious on the cycled graphite anode with PS than PS@COF, suggesting that there are more electrolyte decomposition products on graphite with PS. In the F 1s spectra, the peak at 687.3 eV belongs to LiP_xF_y,[5] and another peak at 685.4 eV is attributed to LiF.[6] In the P 2p spectra the peaks of $LiPO_yF_z$ (134.2 eV) and LiP_xF_y (137.2 eV) can be identified. All these species are derived from electrolyte decomposition and presents stronger peaks on graphite with PS than with PS@COF, confirming the suppression of electrolyte decomposition by PS@COF.

	C	O	F	P	Ni	Co	Mn
Fresh	92%	2%	6%				
PS	18%	10%	33%	19%	5%	4%	11%
PS@COF	54%	20%	16%	10%			

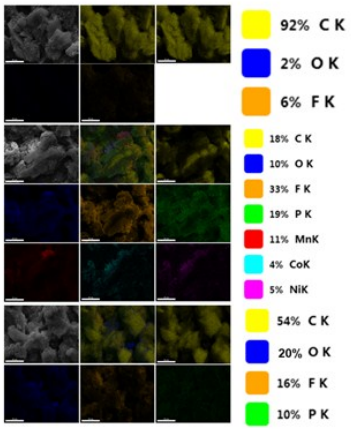

Table S3. The element contents detected on graphite anodes from the Li[$Li_{0.2}Mn_{0.55}Ni_{0.15}Co_{0.1}$]$O_2$/graphite full cells with PS and PS@COF after 100 cycles, determined by mappings.

It can be seen from Table S3 that the content of Ni, Co and Mn on the graphite with PS is sharply increased after cycling, showing that TMIs is free to transport in PS. This case never happens on the graphite with PS@COF, indicating the ability of PS@COF to capture transition metal ions.

References

1. S. Zugmann, M. Fleischmann, M. Amereller, R. M. Gschwind, H. D. Wiemhöfer and H. J. Gores, *Electrochim. Acta*, 2011, **56**, 3926-3933.
2. J. Zhao, L. Wang, X. He, C. Wan and C. Jiang, *J. Electrochemi. Soc.*, 2008, **155**, A292.
3. Y. Lin, X. Yue, H. Zhang, L. Yu, W. Fan and T. Xie, *Electrochim. Acta*, 2019, **300**, 202-207.
4. X. Zheng, X. Wang, X. Cai, L. Xing, M. Xu, Y. Liao, X. Li and W. Li, *ACS Appl. Mater. Interfaces*, 2016, **8**, 30116-30125.
5. Y. Zhu, X. Luo, H. Zhi, Y. Liao and W. Li, *J. Mater. Chem. A*, 2018, **6**, 10990-11004.
6. J. G. Han, S. J. Lee, J. Lee, J. S. Kim, K. T. Lee and N. S. Choi, *ACS Appl. Mater. Interfaces*, 2015, **7**, 8319-8329.